Modeling Laser Guide Star Aberrations

KAON #478

Richard M. Clare and Marcos A. van Dam
W. M. Keck Observatory, 65-1120 Mamalahoa Highway, Kamuela HI 96743
Antonin H. Bouchez
Caltech Optical Observatories, M/S 105-24, Pasadena, CA 91125

Abstract: When using a laser guide star (LGS) adaptive optics system, quasi-static aberrations are observed between the measured wavefronts from the LGS wavefront sensor (WFS) and the natural guide star WFS. We model these LGS aberrations.

OCIS codes: (010.1080) Adaptive optics;(010.7350) Wave-front sensing.

1 Introduction

There are a number of fundamental differences between the wavefront measured with a laser guide star (LGS) in adaptive optics (AO) systems and the actual aberrations to which starlight is subjected. Firstly, it is not possible to determine the tip-tilt (TT) modes from the LGS because the laser is deflected on both the upward and downward paths from the atmosphere. A natural guide star (NGS) is required to estimate these modes. Secondly, because the LGS is located at a finite height (of approximately 90 km) and not at infinity, the LGS sees a cone of turbulence rather than a cylinder. Thirdly, the altitude of the sodium layer is constantly changing, which the LGS wavefront sensor (WFS) sees as a change of focus. The remaining differences are the so-called LGS aberrations [1]. The Keck II laser is projected from the side of the telescope and the LGS WFS is a Shack-Hartmann WFS (the Keck II LGS AO system is described in detail in [1, 2, 3, 4]). For a Shack-Hartmann sensor with a LGS at a finite height and non-zero thickness, the spot at each subaperture is elongated due to the parallax effect. The LGS aberrations arise due to biases introduced by the truncation of these asymmetrically elongated LGS WFS spots by a field stop or pixel boundaries, quad-cell centroiding, and telescope and AO system aberrations [1]. This paper details the modeling of these LGS aberrations and is a summary of the work described in [4].

The LGS aberrations, and also the focus variations due to changes in the altitude of the sodium layer, are measured on the Keck II LGS AO system with the low bandwidth WFS (LBWFS), which guides on the TT NGS. 20% of the light from the TT NGS is passed to the LBWFS, which is a 20×20 Shack-Hartmann WFS, the same order as the LGS WFS. The focus aberration measured by the LBWFS is used to update the LGS WFS focus position, and the higher order aberrations are used to update the reference centroids for the LGS WFS [3]. If the NGS is sufficiently bright ($m_V \leq 18$), the LGS aberrations can be measured

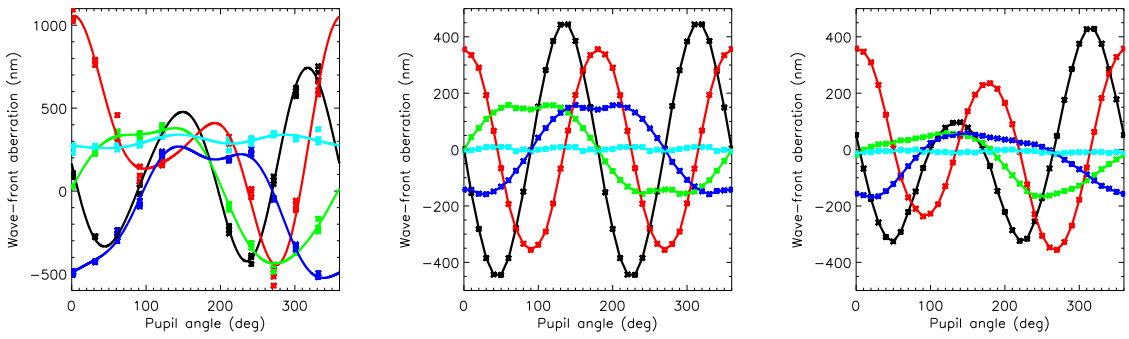

Fig. 1. The LGS aberrations as a function of pupil angle at zenith for (a) measured on sky on 26 January 2005, (b) modeled assuming no UTT error, and (c) modeled assuming an UTT error of (0.″1, -0.″1). The curves are, 0° astigmatism (red), 45° astigmatism (black), y-coma (green), x-coma (dark blue) and spherical aberration (light blue).

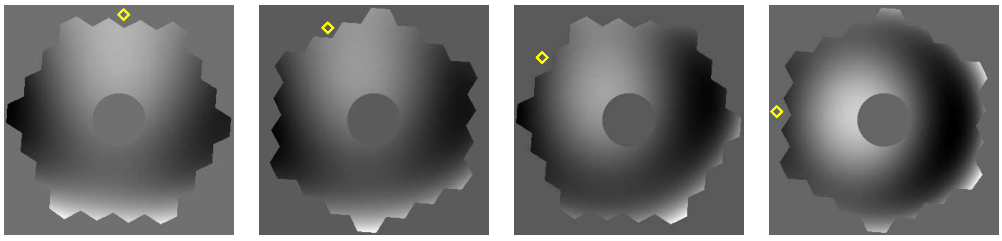

(a) (b) (c) (d)

Fig. 2. The total low order LGS aberrations for the night of 26 January 2005 at a pupil angle of (a) 0°, (b) 30°, (c) 60°, and (d) 90°. The yellow diamond indicates the approximate position of the laser.

with the LBWFS and corrected. If the NGS is fainter than this, or if the telescope pupil is rotating quickly, the LGS aberrations cannot be adequately compensated with the LBWFS alone.

The LGS aberrations were measured on the telescope by locking the TT loop on a bright NGS, and by locking the deformable mirror loop on the LGS and setting the LGS reference centroids to be all zeros. The pupil angle was rotated and LBWFS images taken at regular intervals. The pupil angle thus specifies the position of the laser relative to the WFS subapertures. We will define a pupil angle of 0° to be the laser at the top of the pupil in this paper. The LGS aberrations are calculated as a least-squares fit to the low order Zernike polynomials from the displacements (centroids) of each subaperture of the LBWFS. The first 11 Zernike polynomials (i.e. up to spherical aberration, but ignoring tip, tilt and focus, which are independently corrected, and piston) contain 89% of the mean-squared LGS aberrations. We display the coefficients of the measured LGS aberrations versus pupil angle for the astigmatism, coma, and spherical aberration polynomials for the night of 26 January 2005 in Fig. 1(a). The total low order LGS aberration is shown in Fig. 2 for pupil angles of 0°, 30°, 60°, and 90°.

A number of new LGS AO systems for existing and future telescopes are in the design stages, such as the TMT AO system, NFIRAOS, [5] and the Keck I LGS AO system [6]. In this paper, we model the LGS aberrations observed with the Keck II LGS AO system, and apply this model to current designs for TMT and Keck I LGS AO, and to the existing Palomar LGS AO system [7].

2 Modeling the LGS aberrations

The first step in modeling the LGS aberrations is to calculate the LGS WFS subaperture images. We do this using geometric optics, i.e. ray-tracing. In this model, the LGS images are a function of the launch telescope position, subaperture geometry, zenith angle, atmospheric seeing, size and number of detector pixels, charge diffusion and the sodium profile. The displacement of each LGS WFS subaperture is then calculated as the Fourier shift required to shift the LGS image such that the LGS image has a zero center-of-mass centroid. The LGS aberrations are calculated as a least-squares fit to the low order Zernike polynomials. A representative sodium profile that we use to model the Keck II system was generated as a best fit of the sum of two Gaussians to an acquisition camera image of January 26 2005, the night that the LGS aberrations of Fig. 1(a) were measured.

The modeled LGS aberrations are displayed in Fig. 1(b) for no uplink TT (UTT) error (i.e. the LGS images are correctly centered on the quad-cells). The modeled astigmatism and coma curves are the same periodicity and phase as the measured aberrations of Fig. 1(a). However, unlike the measured aberrations, the magnitude of the modeled astigmatism modes are the same on both cycles, and the coma curves are zero mean.

An UTT error of the laser beam leads to the LGS subaperture images being de-centered with respect to the subaperture optical axis. The effect of the UTT error is to produce a bias in the centroid measurement in the direction of the UTT error. The modeled LGS aberrations for the Keck II system, with an UTT error of 0.″1 in x and -0.″1 in y, are plotted in Fig. 1(c). This combination of UTT x and y error approximately gives the observed behavior of the astigmatism and coma curves in Fig. 1(a).

Table 1. LGS aberrations in Zernike polynomials for the Palomar, Keck I and TMT LGS AO systems.

Zernike polynomial	Coefficient of LGS aberration (nm)		
	Palomar	Keck I	TMT
Z_{11}	5	34	834
Z_{14}	0	25	338
Z_{22}	0	4	42
Z_{26}	0	7	158
Total	5	43	915

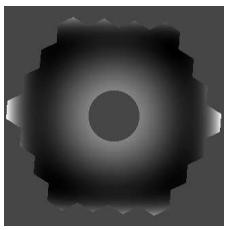

Fig. 3. The simulated total low order LGS aberration for the centrally projected Keck I LGS AO system.

3 Other LGS AO systems

We apply our model for the LGS aberrations to the Palomar LGS AO system [7] (5.1 m diameter), and the planned Keck I [6] (10 m) and TMT LGS AO systems [5] (30 m). In particular, we are interested in determining how the aberrations vary with telescope diameter for these centrally projected laser systems. Because the laser is centrally projected for these three systems, there is no dependence of the aberrations on pupil angle, and instead we tabulate the LGS aberrations for these three systems in Table 1. Most of the low order Zernike coefficients are negligible, so we only tabulate the Zernike polynomials with significant power.

For Palomar, the LGS aberrations at 5 nm are insignificant, due to the central projection of the laser and the small aperture size. For Keck I, the LGS aberrations are significantly less than the side-projected Keck II system. The phase screen represented by the sum of the low order aberrations for Keck I is displayed in Fig. 3. As shown in Table 1, the only non-zero coefficients of the first 30 Zernike polynomials for Keck I and TMT correspond to Zernike polynomials Z_{11} and Z_{22} (circularly symmetric), and Z_{14} and Z_{26} (square symmetric). The circular symmetry arises from the central projection of the laser, and the square symmetry from the square field stop (square extent of the pixels). The total modeled LGS aberration for TMT at 915 nm, is significantly more than the stringent total wavefront error constraint of 133 nm rms [5]. For TMT, the proposed design includes measuring with the TT NGS WFS the focus variations arising from the height of the sodium layer changing [5]. To meet this error requirement, it may be necessary to measure these four higher order terms (Z_{11}, Z_{14}, Z_{22} and Z_{26}) with the fast NGS wavefront sensor.

References

1. M. A. van Dam, A. H. Bouchez, D. Le Mignant and P. L. Wizinowich "Quasi-static aberrations induced by laser guide stars in adaptive optics," Optics Express **14**, 7535-7540 (2006).
2. P. L. Wizinowich et al., "The W. M. Keck Observatory laser guide star adaptive optics system: overview," PASP **118**, 297-309 (2006).
3. M. A. van Dam et al., 'The W. M. Keck Observatory laser guide star adaptive optics system: performance characterization," PASP **118**, 310-318 (2006).
4. R. M. Clare, M. A. van Dam and A. H Bouchez, "Modeling low order aberrations in laser guide star adaptive optics systems," submitted to Optics Express.
5. G. Herriot et al., "NFIRAOS: TMT narrow field near-infrared facility adaptive optics," in *Advances in Adaptive Optics II*, B. L. Ellerbroek, D. Bonaccini Calia eds., Proc. SPIE **6272**, 62720Q (2006).
6. P. L. Wizinowich et al.,"Adaptive Optics Developements at Keck Observatory," in *Advances in Adaptive Optics II*, B. L. Ellerbroek, D. Bonaccini Calia eds., Proc. SPIE **6272**, 627209 (2006).
7. R. Dekany et al., "Laser Guide Star Adaptive Optics on the 5.1 Meter Telescope at Palomar Observatory," AMOS Technical Conference Proceedings (2005).